AFRL-ML-WP-TP-2006-457

SELECTION CRITERIA OF TEST SIGNALS FOR CORRELATION-BASED WIRE FAULT ANALYSIS (PREPRINT)

Venkata Telasula, Dr. Cynthia Furse, and Dr. Chet Lo

MAY 2006

Approved for public release; distribution is unlimited.

STINFO COPY

MATERIALS AND MANUFACTURING DIRECTORATE
AIR FORCE RESEARCH LABORATORY
AIR FORCE MATERIEL COMMAND
WRIGHT-PATTERSON AIR FORCE BASE, OH 45433-7750

REPORT DOCUMENTATION PAGE

Form Approved
OMB No. 0704-0188

1. REPORT DATE *(DD-MM-YY)*	2. REPORT TYPE	3. DATES COVERED *(From - To)*
May 2006	Journal Article Preprint	05/01/2005 – 04/30/2006

4. TITLE AND SUBTITLE
SELECTION CRITERIA OF TEST SIGNALS FOR CORRELATION-BASED WIRE FAULT ANALYSIS (PREPRINT)

5a. CONTRACT NUMBER
FA8650-04-C-5228

5b. GRANT NUMBER

5c. PROGRAM ELEMENT NUMBER
63112F

6. AUTHOR(S)
Venkata Telasula, Dr. Cynthia Furse, and Dr. Chet Lo

5d. PROJECT NUMBER
4130

5e. TASK NUMBER
01

5f. WORK UNIT NUMBER
00

7. PERFORMING ORGANIZATION NAME(S) AND ADDRESS(ES)
University of Utah
Department of Electrical and Computer Engineering
50 S. Campus Drive (3280 Merrill Engineering Building)
Salt Lake City, UT 84112

8. PERFORMING ORGANIZATION REPORT NUMBER

9. SPONSORING/MONITORING AGENCY NAME(S) AND ADDRESS(ES)
Materials and Manufacturing Directorate
Air Force Research Laboratory
Air Force Materiel Command
Wright-Patterson AFB, OH 45433-7750

10. SPONSORING/MONITORING AGENCY ACRONYM(S)
AFRL-ML-WP

11. SPONSORING/MONITORING AGENCY REPORT NUMBER(S)
AFRL-ML-WP-TP-2006-457

12. DISTRIBUTION/AVAILABILITY STATEMENT
Approved for public release; distribution is unlimited.

13. SUPPLEMENTARY NOTES
This work, resulting in whole or in part from Department of the Air Force contract FA8650-04-C-5228, has been submitted to IEEE for publication in the IEEE Sensors Journal. If this work is published, IEEE may assert copyright.
PAO Case Number: AFRL/WS 06-1649, 28 Jun 2006.

14. ABSTRACT
This paper compares reflectometry signals for location of intermittent faults on live electrical cables. STDR, SSTDR, linear chirp, quadratic chirp, concave-up chirp, convex-down chirp and all frequency randomized phase noise signals were tested. The SSTDR was observed to be the most effective signal for live wire testing, because of its minimal interference with the existing signals and narrow correlation signature. This paper provides a methodology for systematically evaluating signal performance and design criteria for live wire test systems.

15. SUBJECT TERMS
Aging wire fault location, Correlation, Reflectometry, Wire faults

16. SECURITY CLASSIFICATION OF:			17. LIMITATION OF ABSTRACT:	18. NUMBER OF PAGES	19a. NAME OF RESPONSIBLE PERSON (Monitor)
a. REPORT	b. ABSTRACT	c. THIS PAGE			Thomas J. Moran
Unclassified	Unclassified	Unclassified	SAR	14	19b. TELEPHONE NUMBER *(Include Area Code)* N/A

Selection Criteria of Test Signals for Correlation-Based Wire Fault Analysis

Venkata Telasula[1], *Student Member*, Dr. Cynthia Furse[1], *Senior Member* and Dr. Chet Lo[1], *Member*

Abstract — **This paper compares reflectometry signals for location of intermittent faults on live electrical cables. STDR, SSTDR, linear chirp, quadratic chirp, concave-up chirp, convex-down chirp and all frequency randomized phase noise signals were tested. The SSTDR was observed to be the most effective signal for live wire testing, because of its minimal interference with the existing signals and narrow correlation signature. This paper provides a methodology for systematically evaluating signal performance and design criteria for live wire test systems.**

Index Terms – **Aging wire fault location, Correlation, Reflectometry, Wire faults.**

I. Introduction

Wiring fault diagnosis is critical for efficient operation and maintenance of electrical systems, especially in aircraft [1]. "Hard faults" such as broken wires or short circuits can be found using many different detection schemes. Smaller faults, particularly intermittent faults that occur in flight but are not reproducible on the ground are a serious maintenance challenge. This paper focuses on methods for detecting and locating these intermittent faults while the aircraft or other system is live and in use. Thus, the fault location method cannot interfere with the existing electrical signals, and those signals must not interfere with proper location of the fault. Several potential methods for intermittent fault location on live systems are compared in this paper.

Intermittent fault location has another very important implication. Maintainers of electrical systems are often interested in knowing the condition of their wiring in order to repair or replace damaged wiring before it causes catastrophic failure. As such, there has been renewed interest in being able to locate small chafes or frays in the wiring. Unfortunately, small damage of this type is notoriously difficult to detect and locate.

For reflectometry test systems, including those that are compared in this paper, a high frequency signal is sent down the wire. Reflections occur at the end of the wire and any large or small impedance changes along its length and return to the testing end of the wire. The reflected signal from a chafe or fray is so small that a very sensitive reflectometer would be needed in order to detect this signal. It has been shown through simulation and measurement that reflections from normal variation on typical uncontrolled impedance wires which make up the majority of wires in aircraft, for instance, are larger than the changes from a chafe or fray. This means that normal variation in the environment can mask a chafe or fray. [2] One way of overcoming this problem would be to record and store a "baseline" of the wire when it is first installed and in perfect condition and then watch for degradation over time. This may be possible in some applications, but in many applications, particularly those with high vibration and temperature changes, the environment is likely to change from the "good" baseline, thus still masking the chafe or fray.

The systems described in this paper that can locate faults while the system is live allow the system to locate the first signs of intermittent faults. The intermittent faults are truly open or short circuits, but for a very short period of time. For this short period of time, they create a large reflection that can be detected over the noise caused by reflection from the normal impedance variation in the wiring system. They may be caused by a wire vibrating against a metal surface, when causing the insulation to be worn away and allowing the exposed conductor to touch the metallic surface, for instance. They might be caused by water breaching radial cracks in brittle wiring insulation.

There are several reasons to believe that locating these kinds of intermittent faults may be effective in reducing the potential for catastrophic failure. Aircraft wire maintainers often report that evidence of short circuits may be noticed during routine maintenance, when no problem was suspected, indicting that there had been a short circuit that went unnoticed and did not cause serious harm. Also, aircraft are built and designed so that a single small spark should not generate a fire or explosion. Numerous events where an arc has occurred, electrical activity has been transferred to a redundant system, and the aircraft has been brought in for repairs, have been noted. Similarly, many cases where multiple intermittent events predate a more serious "hard fault" have been noted. Thus, being able to locate intermittent faults while the system is active may be as or more effective than trying to locate the very small chafes and frays that go along with them.

Reflectometry systems have been shown to be highly effective for locating hard faults on wiring. All of these systems send a high frequency signal down the wire and analyze the reflected signal to determine the distance to the fault and the type of fault. These methods are distinguished by the type of signal and analysis methods they use. Time-Domain Reflectometry (TDR) [3] uses a fast rise time incident pulse and a fast digital sampler for analysis. The time delay and polarity of the reflected

[1] University of Utah, Department of Electrical and Computer Engineering, Salt Lake City, Utah 84112

signal determines the distance to and type of fault, respectively. Frequency Domain Reflectometry (FDR) methods use a sinusoidal test signal and several different methods for analyzing the data. These methods include Phase Detection FDR (PD-FDR) [4], Standing Wave Reflectometry (SWR) [5], and Mixed Signal Reflectometry (MSR) [6]. A combination of these techniques, Time-Frequency Domain Reflectometry (TFDR) has also been proposed. [9] These methods are not ideal for use on live systems, although they may be used in some applications.

Recently several methods for locating faults on live wires have emerged. These include Spectral Time Domain Reflectometry (STDR), Spread Spectrum TDR (SSTDR), [7], and Multicarrier Spread Spectrum (MCSS) [8]. These methods use signals such as pseudo noise codes (STDR), modulated PN codes (SSTDR), or band limited pulses (chirp or MCSS) as the test signals. These signals have less spectral overlap with the existing electrical signals on the live wires being tested than the TDR or FDR signals. They can therefore be used with less interference to or from the existing electrical system. Another method, Noise Domain Reflectometry (NDR) [10], utilizes the existing noise or high frequency signal on the wire as the test signal, thus completely eliminating the possibility of interfering with the existing signals on the line.

The methods described above are correlation-based sensors. Correlation is a measure of how similar two signals are and can be used to tell the precise delay of a signal, such as the reflected signal that is returned from a fault on the wire. Correlation-based delay is used in many other applications including synchronization of wireless communication signals [11], the Global Positioning System (GPS) [12], and pulse-compression "chirp" radar [13]. This paper uses methods developed in these other applications to evaluate the best incident signals for wire fault location.

The performance of a correlation based fault location system is controlled by two aspects of the test signals applied. The first aspect of the test signal is how much it interferes with the existing signal on the live transmission line, and how much the live signal interferes with the test signal. The issue of interference will be evaluated based on existing specifications for allowable noise levels. Although the examples given in this paper are for the specific cases of MIL-STD 1553B and MIL-STD 461E CE102 and RE102 requirements, the assessment method can be readily adapted to other interference requirements. The allowable interference levels will control the allowable magnitude and optimal frequency range for the test signal. This aspect of the test signals will be evaluated in section II

The second important aspect of the test signal is its correlation signature. Narrow correlation signatures are produced by broadband signals and are easier to use and more accurate for fault location. Particularly when analyzing short lengths of wire, where the initial reflection at the start of the wire overlaps the reflection from the end of the wire, narrower correlation signatures produce more accurate results. This aspect of the test signal will be evaluated in section III.

II. Interference and Attenuation Limits

In practice, electromagnetic interference (EMI) standards and high frequency attenuation on the transmission line are the limiting factors for the magnitude and frequency range of the test signals that can be used in correlation-based fault location systems. These limitations also impact the performance of the system, which will be discussed in section III.

The applicable EMI standard for aircraft power lines is the MIL-STD-461E Conducted Emission (CE102) and Radiated Emission (RE102) limit [15]. The limits for 28V DC and 115V 400 Hz aircraft power supply wiring are shown by line (d-e) and (f-g), respectively, in fig. 1. For frequencies below 10 MHz, the CE102 standard (fig.1d and f) limits the amount of voltage that can be directly coupled to the wire under test. For frequencies greater than 10MHz, the RE102 standard (fig 1e and g) is applied. The RE102 standard, expressed in dBμV/m, limits power radiated from the system, which depends on the signal on the wire as well as the layout and environment, lengths of wires, etc. Since the objective of the paper is to compare different types of fault location the RE102 limit level was assumed to be continuous with CE102 as shown in fig.1, although in practice this is not necessarily the case.

MIL-STD 1553B [17] is the applicable EMI standard for aircraft digital data lines. This standard limits worst-case additive white Gaussian (AWG) noise to 140mV RMS from 1 kHz to 4MHz for a terminal with a transformer coupled stub. This is shown in fig. 1c.

Transmission lines are inherently lossy at high frequencies, and this attenuation profile makes them effectively low pass filters and limits the maximum test frequency that can be used. The filter profile depends on

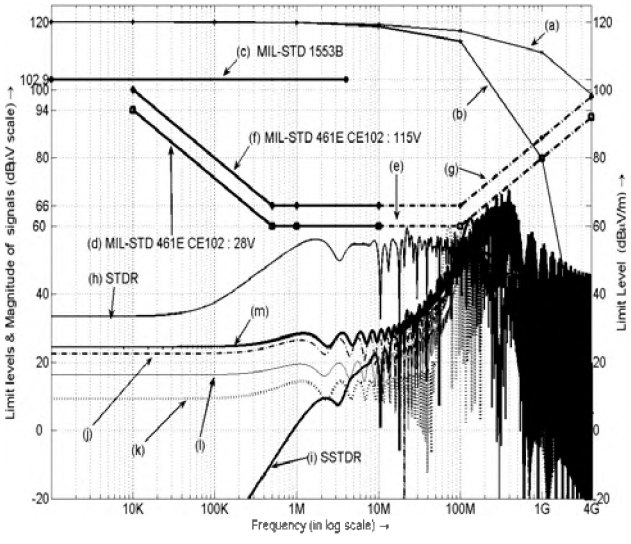

Fig. 1. EMI Standards, attenuation curves, and spectral content of test signals (a) Attenuation for 100' of RG58 coaxial line, (b) Attenuation for 100' of two wire line, (c) MIL-STD 1553B, (d) MIL-STD 461E CE102 for 28V DC lines, (e) MIL-STD 461E RE102 assumed continuous with the CE102 standard, (f) MIL-STD 461E CE102 for

115V 400 Hz lines, (g) MIL-STD 461E RE102 continuation of CE102 standard, (h) STDR (127 chips, 300 MHz), (i) SSTDR (127chips, 300MHz), (j) linear chirp (100- 400MHz, time-width of 0.42μs (k) quadratic chirp (l) concave-up chirp (m) convex-down chirp

the type and length of transmission line and is shown for a 100-ft RG 58/U coaxial transmission line (inner conductor radius of 0.51mm, outer conductor radius of 1.96mm, polyethylene insulation) in fig.1(a) and for a 100-ft two-wire transmission line (inner conductor radius of 0.511mm, distance between the center of the two conductors of 2.54mm, and PVC insulation) in fig. 1(b).

The combination of attenuation and EMI standards controls the frequency profile of the signal that can be placed on the line. The signal must effectively propagate to the end of the wire and back (attenuation) without interfering with the aircraft (EMI) and without having the aircraft interfere with the test signal. The next section describes the nature of the correlation of different test signals and what aspects of the correlation are important for optimal fault location.

III. Correlation Signatures

A transmission line carries a real signal $g(t)$ and some noise $n(t)$. A test signal, $f(t)$, is added to the signal on the line. The test signal travels down the line a distance d to the fault and returns with a time delay $\tau_1/2$. It may also experience some attenuation a. The reflected signal can be then represented as $f_{2d}(t) = a \bullet f(t-\tau_1)$. Correlation-based test systems can either sample the signals and perform the correlation in software [10], or they can perform the correlation in hardware [7-9]. The correlation signature $c(\tau)$ can be defined as

$$c(\tau) = \frac{1}{c(0)} \int_{t+nT}^{\tau+(n+1)T} (g(t) + f(t) + af(t-\tau_1) + \ldots n(t)) \bullet f(t-\tau)\,dt \quad (1)$$

where the correlation for each delay τ is normalized by $c(0)$. [7] A typical correlation waveform can be seen in fig. 2. that the correlation includes a non-zero cross-correlation between $g(t)$ and $f(t-\tau)$ which can be minimized by designing the signal $f(t)$ such that it is orthogonal to $g(t)$. When testing dead (unpowered) lines, $g(t) = 0$, and the cross correlation is zero. The cross-correlation between noise $n(t)$ and $f(t-\tau)$ can also be minimized by designing the signal $f(t)$ to be minimally susceptible to noise.

An ideal correlation function $c(\tau)$ for fault location is an impulse function, and its corresponding power spectrum $C(\omega)$ is uniform over the infinite frequency range. The attenuation and EMI limits shown in Figure 1 limit the frequency range of the test signal $F(\omega)$. This causes broadening of the correlation peak and the appearance of side lobes, which limit the effectiveness of peak detectors for location of the peaks and hence the faults. This problem is further exacerbated by multiple overlapping reflections commonly seen in wiring systems, such as multiple reflections between the source and load, branched networks, and multiple faults [18].

Three major parameters determine the accuracy and effectiveness of a correlation-based fault system: (a) Interference (cross correlation) between the existing signals, $g(t)$ and test signal, $f(t)$, (b) detectability of the peak of the correlation between $f(t)$ and $f(t-\tau)$, and (c) resolvability of multiple correlation peaks.

The resolvability of the correlation waveform $c(\tau)$ using a simple peak detector is characterized for this paper in terms of the 6-dB main lobe width, zero-crossing main lobe width, the strength of the first side lobe level, the location of the first side lobe level, and the interference from the test signal. Fig. 2 illustrates these parameters. The 6-dB main lobe width specifies the distance beyond which two correlation waveforms add coherently to a single main lobe peak. Minimizing the side lobes minimizes overlap between adjacent correlation peaks and therefore enhances resolvability.

The interference between the investigation signal $f(t)$ and the existing signal $g(t)$ is also an important parameter in live wire testing. $F(\omega)G(\omega)$ should be minimized over the dominant frequency range of $g(t)$. Electromagnetic Interference (EMI) specifications determine the maximum allowable interference for a specific application. Another measure of resolvability is the time-resolution constant $T_c(0)$:

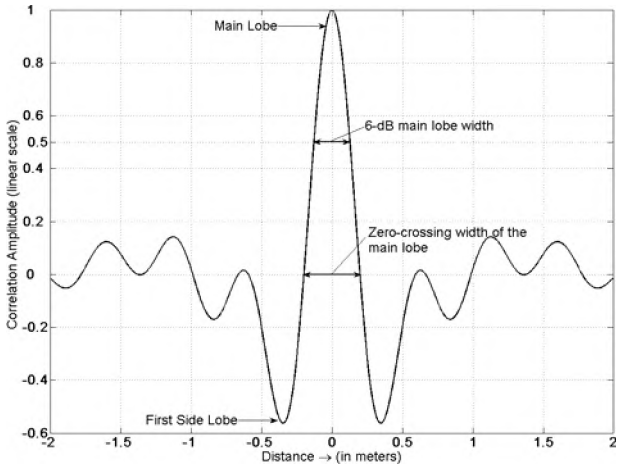

Fig.2. Typical correlation waveform. The different parameters used for performance comparison are shown.

$$T_c(0) = \frac{\int_{-\infty}^{\infty} |c(\tau)|^2 \, d\tau}{|c(0)|^2} \quad (2)$$

The smaller the time-resolution constant, the better the system can resolve multiple peaks. [13]

IV. Potential Signals for Correlation-Based Fault Location

This section evaluates a number of potential test signals for correlation-based fault location including (a) Sequence Time Domain Reflectometry (STDR), (b)

Spread Spectrum Time Domain Reflectometry (SSTDR), (c) linear chirp, and non-linear chirp signals with their time-frequency distributions as (d) quadratic, (e) Concave-up, and (f) Convex-down.

It is well known that maximizing the bandwidth of the signal will provide the best correlation waveform for fault location, although this must be tempered somewhat by the potential interference between the test signal and existing signals on the wire. The EMI standards described in section II ensure that the test signals will not interfere with the aircraft. They also specify the maximum "noise" signal that will be present in addition to the expected signal on the aircraft. The combination of the noise and data signals gives the maximum interference with the test signal.

In addition to ensuring that the test signal does not interfere with the aircraft signal and vice versa, it is also desirable to have a narrow correlation signature with minimal sidelobes for accurate fault location. For comparing the correlation waveform, the investigation signals are of the same time duration and band-width but of different shapes. The bandwidth of the chirp could be defined several different ways. In this paper, it was defined as the difference between maximum and minimum frequencies in the chirp generation. The correlation analysis has been performed in an unpowered and noise-free environment where $g(t)=0$ and $n(t)=0$. The velocity of propagation υ_p associated with the transmission line is assumed to be constant over the entire range of frequencies, and the value is taken as the Kuzniar Number $\upsilon_p = 2/3 * 2.99998 \times 10^8$ m/s.

A closed-form analytical formulation of all of these correlation waveforms is not available. Thus, correlation waveforms were found numerically and are shown in fig. 4 and summarized in table I for each of the signals described in this section. The frequency spectra of the signals are shown in fig.1.

A. Sequence Time Domain Reflectometry (STDR) signal

The STDR signal [7] is an n-stage Maximum Length (ML) Pseudo Noise (PN) sequence. The main lobe of the correlation waveform resembles a triangular peak spread over two chip lengths of the PN sequence as shown in fig. 4. For this example, a 12mVpp, zero-centered 300MHz 7-stage (127 chips long) PN code was used. The magnitude is limited by the CE/RE102 standard as shown in Fig.1. The PN code generator was assumed to be ideal with zero rise time and no internal noise. The 6-dB main lobe width, zero-crossing main lobe widths and the location of the first side lobe peak with respect to the main lobe peak of the STDR signal are inversely proportional to the signal frequency. The strength of the first side lobe with respect to the main lobe peak is invariant to the increase in the signal frequency. As shown in Table I, the time-resolution constant of the STDR signal is high compared to the other test signals. This can be attributed to the non-uniform, *Sinc*-type envelope associated with the frequency magnitude of the STDR signal. The time-resolution constant of the STDR signals decreases as the frequency is increased, because the frequency spectrum of the STDR signal broadens.

B. Spread Spectrum TDR (SSTDR) signal

The SSTDR signal [7] is a sine wave modulated STDR signal. The SSTDR signal used in this example is the STDR signal multiplied by a 300 MHz sinusoidal signal, limiting the peak-peak amplitude to 72mV, as per CE102/RE102 requirement. Similar to STDR, the 6-dB main lobe width, zero-crossing main lobe width, location of the first side lobe peak with respect to the main lobe peak are inversely proportional to the signal bandwidth. The strength of the first side lobe with respect to the main lobe peak is invariant to the increase in the signal bandwidth. The time-resolution constant of the SSTDR signal decreases with the square of the change in signal bandwidth.

C. Linear Chirp Signal

The linear chirp is a frequency modulated signal often used in radar [2]. A linear chirp can be represented as

$$f(t) = A\cos\left(2\pi * f_i(t) * t\right) \tag{3}$$

where

$$f_i(t) = f_0 + \frac{\mu}{2} * t \tag{4}$$

$$\mu = \frac{f_1 - f_0}{t_1} \tag{5}$$

in which $A = 20.5mV$ is the amplitude of the chirp, limited by the CE/RE102 standard as shown in Fig.1. $f_0 = 100\text{MHz}$ is the start frequency of the linear chirp at time $t = 0$, and $f_1 = 400\text{MHz}$ is the end frequency of the linear chirp at time $t_1 = 0.42\mu$ seconds, the duration of the signal. The distribution of $f_i(t)$, instantaneous frequency, with respect to time t can be seen in fig. 3. The linear chirp features a flat frequency spectrum that decreases rapidly outside the band of interest. The techniques for generating a linear chirp are widely discussed in the literature [13]. The orthogonal nature of the chirp signal with respect to the delayed version of the same chirp signal arises from the use of a time-frequency distribution in the chirp generation. The 6-dB main lobe width, zero-crossing main lobe width, the location of the first side lobe peak with respect to the main lobe peak vary inversely proportional to the square root of the bandwidth. The strength of the first side lobe peak varies in proportion to the bandwidth of the signal. The time-resolution constant varies inversely with the square of the change in bandwidth.

D. Quadratic Chirp Signal

The quadratic chirp is generated as in (3) with $f_i(t)$ defined as

$$f_i(t) = f_0 + \frac{\mu}{3}\left(t - \frac{t_1}{2}\right)^2 \text{ for } t \geq \frac{t_1}{2} \tag{6}$$

For $t < \frac{t_1}{2}$, $f_i(t)$ is the left-to-right flipped version of $f_i(t)$ for $t \geq \frac{t_1}{2}$.

$$\mu = \frac{f_1 - f_0}{t_1^2} \tag{7}$$

where $f_0 = 100\text{MHz}$ is the frequency at time $t_0 = t_1/2 = 0.21\mu\text{s}$ and $f_1 = 400\text{MHz}$ is the frequency at time $t_1 = 0.42\mu\text{s}$. The amplitude of the chirp is $\text{A} = 8.7m\text{V}$. The time-frequency distribution with the above parameters can be seen in fig. 3. The correlation waveforms exhibit very low first side lobe strength compared to the other signals. The 6-dB main lobe width varies as the square root of the bandwidth of the chirp signal. The location of the first side lobe moves away from the main lobe peak as the bandwidth of the chirp increases. The strength of the first side lobe level decreases linearly with the bandwidth. The time-resolution constant of the quadratic chirp varies inversely to the square of the change in bandwidth.

E. Concave-up Chirp Signal

The concave-up chirp is generated as in (3), with a time-frequency distribution defined as

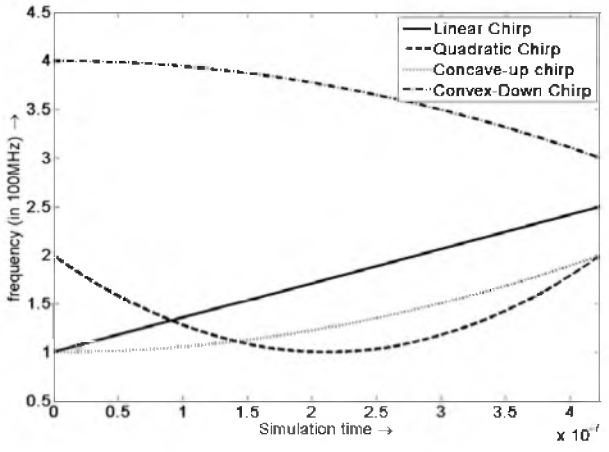

Fig. 3. Time-frequency distributions of chirp signals.

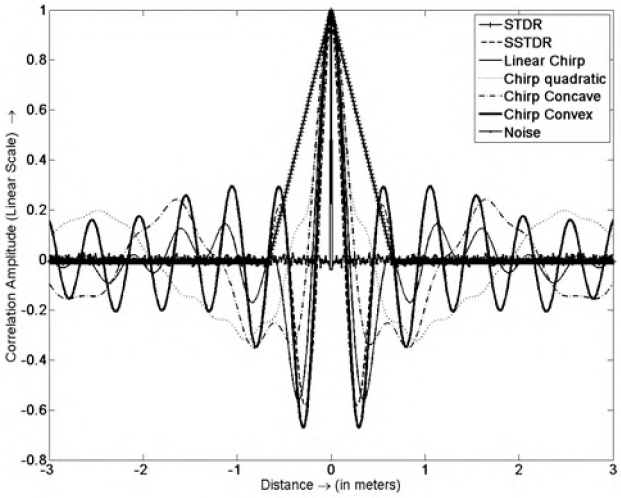

Fig. 4. Correlation waveforms of the various signals investigated. The figure shows that the main lobe of STDR is spread over greater distance compared to the others .

$$f_i(t) = f_0 + \frac{\mu}{3}t^2 \tag{8}$$

where μ is as defined in (7), $f_0 = 100\text{MHz}$ is the start frequency at time $t = 0$, and $f_1 = 400\text{MHz}$ is the end frequency at time $t_1 = 0.42\mu\text{s}$. The amplitude of the chirp signal is $\text{A} = 9.7m\text{V}$. The time- frequency distribution of the concave-up chirp signal is shown in fig. 3. The 6-dB main lobe width decreases linearly with the bandwidth. The location of the first side lobe with respect to the main lobe peak varies inversely proportional to the square root of the bandwidth. The strength of the first side lobe peak decreases linearly with the bandwidth. The time-resolution constant is inversely proportional to the square of the change in bandwidth.

F. Convex-Down Chirp Signal

The convex-down chirp is generated as in (3), with a time-frequency distribution described in (8) where $f_0 = 400\text{MHz}$ is the start frequency at time $t = 0$, and $f_1 = 100\text{MHz}$ is the end frequency at time $t_1 = 0.42\mu\text{s}$. The amplitude of the chirp signal is $\text{A} = 33.5m\text{V}$ .The time-frequency distribution of the convex-down chirp signal is shown in fig. 3. The 6-dB main lobe width, zero-crossing main lobe width, and location of the first side lobe peak with respect to the main lobe peak are inversely proportional to the square root of the bandwidth. The time-resolution constant is inversely proportional to the square of the change in bandwidth.

G. All Frequency Randomized Phase Noise Signal

An all frequency randomized phase noise signal has a spectral content that occupies all frequencies with magnitudes limited by the interference limits. With MIL-STD 461E CE102 and RE102 requirements for a 28V aircraft power cables, an all frequency randomized phase noise signal was generated. The correlation waveform of the signal exhibits very sharp correlation peaks. The 6-dB main lobe width, zero-crossing width and location of the first side lobe level for the signal were limited by the

differential delay used in computing the correlation waveform. A typical correlation waveform in this case can be seen in fig. 4. The RMS value of the randomized phase noise signal with respect to 28V aircraft power cable with MIL-STD 461E requirement was found to be 56.59mV and for 115V aircraft power cable, it was found to be 113.18mV. Although the all frequency randomized phase noise signal is an optimal signal for wire testing, if the presence of external noise combined with the test signal exceeds the prescribed interference limits, design of the test signal in the frequency domain may not be feasible.

V. Comparison of Signals for Correlation-Based Fault Location

Each of the different signals used for correlation-based fault location have different tradeoffs between interference and resolvability.

A. Magnitude of the Test signal vs. Interference limit

Electromagnetic interference specifications limit the interference between the test signals and the existing signals on the aircraft, which also effectively limits the magnitude of the test signals that can be injected onto the wire. The test signals shown in fig. 1 are scaled to meet the interference limits for 28V aircraft power lines. The 300MHz SSTDR signal is the best choice of the signals presented. For applications with different EMI and attenuation limits, the optimal signal may be different.

B. Fault resolvability

Once the signal has been adjusted to meet the EMI requirements, the next parameter to consider is the resolvability of the correlation function, as defined by the time-resolution constant given in (2). The time-resolution constant shows that if the spectrum of the test signal is uniform over a large band, the correlation peak will be narrower. The chirp signals satisfy this criterion and hence have narrower correlation peaks than those of STDR signals. The side lobe levels of the correlations of the chirp signals also have very low side lobe levels, and the location of the first side lobe peak is far from the main lobe peak. This characteristic will be useful in the case of closely spaced faults, which create overlapping correlation peaks. Of all the signals considered, the quadratic chirp signal has the farthest first side lobe location, and STDR has the best first side lobe strength.

In the case of a single fault, the SSTDR was found to be the best choice of the signals considered due to its low interference levels in the low frequency region. In the case of multiple overlapping faults, the quadratic chirp is the best signal to use because of its low first side lobe level that will reduce overlaps between reflections from different faults.

For all methods described in this paper, use of higher bandwidth increases the resolvability of the correlation peak (and hence the accuracy of the method), so it is best to use the maximum bandwidth possible for the application of interest. This will depend on the EMI standard and the attenuation, which depends on the wire type and length.

VI. Conclusion

The ability to locate faults on live wires is important in order to find intermittent faults, which are among the most expensive and time consuming electrical problems to diagnose and repair. Several methods of locating faults on live wires have previously been developed (STDR and SSTDR), and this paper evaluates those functions as well as several chirp functions. The narrowness and shape of the correlation peaks and the interference with/by the aircraft signals control the resolvability and hence accuracy of the signals and the magnitude of the signal that can be used.

The observations made with respect to resolvability and interference limits can be summarized as follows:

1) Increased bandwidth for all methods provides better resolvability.

2) As previously noted [7], SSTDR provides less interference and better resolvability than STDR. In general, SSTDR was found to be better than the chirps introduced in this paper, although is some specific instances or applications, a chirp may be better, particularly for resolving closely spaced reflections.

3) The RE102 limit gives the limiting magnitude of the SSTDR and chirp signals. STDR is limited by the CE102 standard. Since the RE102 limit is based on radiated fields, which are dependent on the environment, the exact magnitude of the signals should be evaluated experimentally or with detailed simulation for their specific environment. Additional power could be allowed in the SSTDR and chirp signals in some cases.

Of the STDR, SSTDR, linear chirp, quadratic chirp, concave-up chirp, convex-down chirp and all frequency randomized phase noise signals tested in this paper, the SSTDR was observed to be the most effective signal for livewire testing, because it had the least interference with the existing signals on the wires and also the correlation signature that gave the most resolvability of the fault location. Additional test signals are likely to emerge over the next few years. This paper provides a methodology for systematically evaluating their performance and design criteria for livewire test systems.

Acknowledgements

This work was supported by the United States Air Force Research Labs through a subcontract from Iowa State University under Contract FA8650-04-C-5228. We would also like to thank, Dr. Paul Smith of LiveWire Test Labs Inc., for his insight in our understanding of the MIL-STD 461E specifications.

References

[1] C. Furse and R. Haupt, "Down to the wire", *IEEE Spectr.*, vol. 38, no. 2, pp. 34-39, Feb. 2001
[2] Lance Griffiths, Rohit Parakh, Cynthia Furse, Brittany Baker, "The Invisible Fray: A Critical Analysis of the Use of Reflectometry for Fray Location," *IEEE Journal of Sensors*, June 2006
[3] Hewlett-Packard , TDR Fundamentals, HP Application Note 62, p 57, 1988
[4] C. Furse, Y. C. Chung, R. Dangol, M. Nielsen, G. Mabey, R. Woodward, "Frequency Domain Reflectometry for On Board Testing of Aging Aircraft Wiring," *IEEE Trans. Electromagnetic Compatibility, p.306-315.*, May 2003
[5] F. T. Ulaby, *Fundamentals of Applied Electromagnetics,* Prentice Hall, 2001
[6] P. Tsai, C. Lo, Y. C. Chung, C. Furse, "Mixed-Signal Reflectometry for Location of Faults on Aging Wiring", I*EEE Journal of Sensors,* pg. 1479 – 1482, Dec. 2005
[7] P. Smith,C.Furse, J.Gunther, "Fault Location on Aircraft Wiring Using Spread Spectrum Time Domain Reflectometry," *IEEE Journal of Sensors,* Vol.5, No. 6, Dec. 2005, pp. 1469-1478
[8] B. Farhang-Boroujeny and C. Furse, "Robust Multicarrier Spread Spectrum Technique for Data Transmission over Partially Jammed Channels," *IEEE Transactions on Signal Processing*, Vol. 53, No. 3, pp. 1038-1044, March 2005
[9] Y.J. Shin, T. Choe, E. Song, J. Park, J. Yook, and E. J. Powers, "Application of Time-Frequency Domain Reflectometry for Detection and Localization of a Fault on a Coaxial Cable", *IEEE Transactions on Instrumentation and Measurement,* Vol. 54, No. 6, pp. 2493-2500, December 2005.
[10] C. Lo, C. Furse, "Noise Domain Reflectometry for Wire Fault Location," *IEEE Transactions on EMC*, pp.97-104, Feb. 2005,
[11] H. Meyr, M. Moeneclaey, S. A. Fechtel, *Digital Communication Receivers, Vol. 2: Synchronization, Channel Estimation, and Signal Processing* Wiley-Interscience , 1997
[12] A. El-Rabbany, *Introduction to GPS: The Global Positioning System,* Artech House Publishers 2002
[13] C. E. Cook and M. Bernfeld, *Radar Signals : An Introduction To Theory And Application,* Academic Press, 1967
[14] THIS REFERENCE NOT USED?? Probably not needed, please check all references are used.W. W. Jones and K R Jones, "Sequence time domain reflectometry for DSL diagnostics", *Electronic Engineering*, June 2001
[15] Department of Defense, Interface Standard, Requirements for the Control of Electromagnetic Interference Characteristics of Subsystems and Equipment, [http://www.jsc.mil/jsce3/emcslsa/stdlib/docs/MilStd/MIL-STD-461E.pdf], Aug 1999.
[16] E. Bogatin, "Signal Integrity: Simplified", Prentice Hall, 2004.
[17] *MIL-STD-1553 Designer's Guide,* pp. II-28 to II-48, New York: ILC Data Device Corporation, 1998, 6th Ed.
[18] Cynthia Furse, Chet Lo, You Chung Chung, Paul Smith, Praveen Pendayala, Kedarnath Nagoti, "Spread Spectrum Sensors for Critical Fault Location on Live Wire Networks," *Journal of Structural Control and Health Monitoring*, Vol 12: pp. 257-267, 2005

	STDR	SSTDR	Linear Chirp	Quadratic Chirp	Concave-up Chirp	Convex-down Chirp	All frequency Noise
Time -resolution constant	2.231E-09	1.1585E-09	1.6895E-09	3.2712E-09	2.598E-09	2.635E-09	1.0263E-10
6-dB width of main lobe (in meters)	0.66	0.16	0.26	0.3	0.32	0.22	0.02
Zero-crossing main lobe width (in meters)	1.3	0.28	0.4	0.9	0.5	0.32	0.02
Strength of the First side lobe peak	-42.08	-4.70	-4.992	-9.786	-9.404	-3.478	-28.11
Location of first side lobe (in meters)	0.66	0.28	0.35	0.9	0.42	0.3	0.01
MIL-STD 461 CE 102: 28V power lines Magnitude of the signal (mV)	12 (p-p)	72 (p-p)	20.5	8.7	9.7	33.5	56.59 (RMS)
MIL-STD 461 CE 102: 115V power lines Magnitude of the signal (mV)	24 (p-p)	144 (p-p)	41.0	17.4	19.4	67.0	113.18 (RMS)
MIL-STD 461 CE 102: 28V power lines Magnitude of the signal[1] (mV)	13 (p-p)	80 (p-p)	39.0	14.5	17.0	45.0	56.59 (RMS)
MIL-STD 1553B: maximum p-p value that can be used (mV) (Transformer-coupled stub)	200	200	200	200	200	200	200
MIL-STD 1553B: maximum p-p value that can be used (mV) (Direct-coupled stub)	280	280	280	280	280	280	280

TABLE I: VARIOUS PARAMETERS USED IN THE SELECTION OF INVESTIGATING SIGNALS IN LIVE-WIRE TESTING; STDR SIGNAL IS OF 127 CHIP LENGTH AND CHIP RATE 300MHZ; SSTDR IS OF 127CHIP LENGTH AND CHIP AND SINUSOIDAL RATE OF 300MHZ; LINEAR, QUADRATIC, CONCAVE-UP AND CONVEX-DOWN CHIRPS EXTENDS FROM 100MHZ TO 400MHZ AS DEFINED IN FIG.4; ALL FREQUENCY NOISE IS MADE OF ALL THE ALLOWABLE FREQUENCIES WITHIN THE INTERFERENCE LIMITS; IN THE CASE OF SIGNAL[1] , STDR SIGNAL IS OF 127 CHIP LENGTH AND CHIP RATE 350MHZ; SSTDR IS OF 127CHIP LENGTH AND CHIP AND SINUSOIDAL RATE OF 350MHZ; LINEAR, QUADRATIC, CONCAVE-UP AND CONVEX-DOWN CHIRPS EXTENDS FROM 200MHZ TO 500MHZ;